Available online at www.sciencedirect.com
SCIENCE DIRECT
Journal of Physics and Chemistry of Solids 67 (2006) 150–153
JOURNAL OF PHYSICS AND CHEMISTRY OF SOLIDS
www.elsevier.com/locate/jpcs

Spectra of the high T_c cuprates understood by the variational studies of the t–J-type models

T.K. Lee [a], C.T. Shih [b], Chang-Ming Ho [c,*]

[a] *Institute of Physics, Academia Sinica, Nankang, Taipei, Taiwan 11529*
[b] *Department of Physics, Tunghai University, Taichung, Taiwan 40744*
[c] *Department of Physics, Tamkang University, Tamsui, Taiwan 25137*

Abstract

Trial wavefunctions with and without antiferromagnetic order for the 2-dimensional t–J-type model are proposed to describe the low-energy states of high T_c cuprates with doped holes or electrons. In the slightly doping regime, we found states behaving like charged quasi-particles with well-defined momenta and having much less pairing correlations than previously studied ones. There exist also states showing the incoherent and 'spin-bag' behaviors. Our results are supported by exact calculation and are consistent with recent photoemission experiments. With increasing doping, superconducting states emerge and behave similarly with that described in recent band-structure analysis and seen in various materials.

Continuous improvement of angle-resolved photoemission spectroscopy (ARPES) and sample making have made possible the detailed study of the spectra in high T_c cuprates [1]. Indeed, many intriguing behaviors relating the physics of doping the two-dimensional Mott insulator in the very underoped regime are observed, e.g. recent ARPES reveals contrasting behaviors between lightly hole- and electron-doped [e.g. $Nd_{2-x}Ce_xCuO_2$ (NCCO)] high T_c cuprates [1,2]. While a small hole patch is observed to be around the center in the nodal direction of the Brillouin zone (BZ) [i.e. $(\pi/2,\pi/2)$] in lightly hole doped systems, small electron patches centered at $(\pi,0)$ and $(0,\pi)$ in lightly doped NCCO. In systems with more doped holes, the doping dependence of photoemission results around the anti-nodal region were also shown to vary in materials with different T_c [1,3].

To understand these experiments, we discuss our recent proposal of a theory based on the variational Monte Carlo (VMC) approach to extract the spectra of the models [4–8] and to compare with the existing various numerical techniques, such as exact diagonalization (ED) studies, self-consistent Born approximation (SCBA) and the Green function Monte Carlo method (see [4,5] and references therein) for the t–J-type models. Specific trial wavefunctions (TWF's) describing well the low-energy states of the associated t–t'–t''–J model Hamiltonian with lightly and overdoped doped holes and/or electrons give results reminding that observed in real materials.

We consider the t–J-type Hamiltonian $\boldsymbol{H} = \sum_{\langle i,j\rangle\sigma} -t_{ij}\tilde{c}^{\dagger}_{i\sigma}\tilde{c}_{j\sigma}$ +H.C. + $\boldsymbol{H}_J$ in which $\langle i,j\rangle$ represents nearest-neighbor (n.n) sites the electron hops (with amplitude t), second n.n. (t'), third n.n. site (t'') pairs and $\boldsymbol{H}_J = J\sum_{\langle i,j\rangle}(\mathbf{S}_i\cdot\mathbf{S}_j - (1/4)n_in_j)$. Note that $\tilde{c}_{i\sigma}$ in $\boldsymbol{H}$ can be viewed to create different kinds of *holes* from single-electron-occupied sites at half-filling: *empty holes* (0*e*-hole) for hole doping and *two-electron-occupied holes* (2*e*-hole) for electron doping [9]. Operator $\tilde{c}_{i\sigma}$ is actually equal to $c_{i\sigma}(1-n_{i,-\sigma})$ or $c_{i-\sigma}n_{i,\sigma}$ for hole or electron doped case, respectively. Therefore, despite the constraints, states in the two cases are in one-to-one correspondence after a local transformation $c_{i\sigma}\rightarrow c^{\dagger}_{i,-\sigma}$ is made. Also, because of the Fermi statistics, the exchange of a single spin with a 2*e*-hole has an extra *minus* sign as compared to the 0*e*-hole. Hence, the only difference between the hole and electron doped t–t'–t''–J model is $t'/t\rightarrow -t'/t$ and $t''/t\rightarrow -t''/t$ after we change the $c_{i\sigma}$ on B sublattice sites to $-c_{i\sigma}$ [10]. With all these, we then treat the hole and electron doped cases in the same manner. The VMC results presented in this paper are for $J/t=0.3$, $t'/t=-(+)0.3$ and $t''/t=+(-)0.2$ in the hole(electron) doped case following the values usually used [10].

The TWF's, in the form of the resonating-valence-bond (RVB) state by Anderson [11], we constructed may include three mean-field paramters depending on the doping concentration: the staggered magnetization $m_s = \langle S^z_A\rangle = -\langle S^z_B\rangle$, where the lattice is divided into A and B sublattices when

* Corresponding author.
E-mail address: dominus@mail.tku.edu.tw (C.-M. Ho).

0022-3697/$ - see front matter © 2006 Elsevier Ltd. All rights reserved.
doi:10.1016/j.jpcs.2005.10.049

antiferromagnetic long range order (AF LRO) is present; the uniform bond order parameters $\chi = \langle \sum_\sigma c^\dagger_{i\sigma} c_{j\sigma} \rangle$; and d-wave RVB (d-RVB) order $\Delta = \langle c_{j\downarrow} c_{i\uparrow} - c_{j\uparrow} c_{i\downarrow} \rangle$ if i and j are n.n. sites in x-direction and -Δ in y-direction. In the following, we discuss these WF's at different doping regimes.

Lightly doped regime. The WF's for lightly doped case are generalizations of the single-hole WF with explicit AF LRO first proposed by Lee and Shih [12]. In contrast to other TWF's [13], ours are constructed solely from the optimized one at half-filling

$$|\Psi_0\rangle = P_e \left[\sum_{\mathbf{k}} (A_{\mathbf{k}} a^\dagger_{\mathbf{k}\uparrow} a^\dagger_{-\mathbf{k}\downarrow} + B_{\mathbf{k}} b^\dagger_{\mathbf{k}\uparrow} b^\dagger_{-\mathbf{k}\downarrow}) \right]^{N_s/2} |0\rangle$$

which does not contain any information about hoppings, t', t'' and neither explicitly t, of the doped hole or electron. However, the effect of t is included in the RVB uniform bond χ which describes the large quantum fluctuation and spin singlet formation. There is also no need to introduce t' and t'' in the TWF as they here are compatible with AF LRO. Coefficients $A_{\mathbf{k}}$ and $B_{\mathbf{k}}$ are functions of $\xi_{\mathbf{k}}$ and $\Delta_{\mathbf{k}}$. $\pm\xi_{\mathbf{k}} = \pm(\varepsilon^2_{\mathbf{k}} + (Jm_s)^2)^{1/2}$ are energy dispersions for the two spin density wave (SDW) bands with $c_{\mathbf{k}} = -(3/4)J\chi(\cos \mathbf{k}_x + \cos \mathbf{k}_y)$. $a_{\mathbf{k}\sigma}$ and $b_{\mathbf{k}\sigma}$ represent the operators of the lower and upper SDW bands, respectively, and are related to the original electron operators $c_{\mathbf{k}\sigma}$ and $c_{\mathbf{k}+\mathbf{Q}\sigma}$ with $\mathbf{Q} = (\pi,\pi)$ set for the commensurate SDW state. $\Delta_{\mathbf{k}} = (3/4)J\Delta d_{\mathbf{k}}$ with $d_{\mathbf{k}} = \cos \mathbf{k}_x - \cos \mathbf{k}_y$ here is for the d-RVB order parameter. The projection operator P_e enforces the constraint of one electron per site. At half-filling, N_s(number of sites) equals the total number of electrons. Notice that the sum in $|\Psi_0\rangle$ is taken over sublattice BZ (SBZ). There are two variational parameters: Δ/χ and m_s/χ in these WF's.

When a hole is doped or an electron is removed from $|\Psi_0\rangle$, a pair must be broken with an unpaired spin left. Thus it is quite natural to have the following WF for a single doped hole, e.g. with a lone up spin

$$|\Psi_1(\boldsymbol{q}_s)\rangle = P_d c^\dagger_{\mathbf{q}_s\uparrow} \left[\sum_{[\boldsymbol{k}\neq\boldsymbol{q}_h]} (A_{\boldsymbol{k}} a^\dagger_{\boldsymbol{k}\uparrow} a^\dagger_{-\boldsymbol{k}\downarrow} + B_{\boldsymbol{k}} b^\dagger_{\boldsymbol{k}\uparrow} b^\dagger_{-\boldsymbol{k}\downarrow}) \right]^{(N_s/2)-1} |0\rangle,$$

where the hole momentum $\boldsymbol{q}_h$ is excluded from the sum if $\boldsymbol{q}_h$ is within the SBZ, otherwise, $\boldsymbol{q}_h$-$\mathbf{Q}$ is excluded. P_d here enforces the constraint of no doubly occupied sites. When we choose the unpaired-spin momentum $\mathbf{q}_s$ to be either the same as the hole momentum $\boldsymbol{q}_h$ or $\boldsymbol{q}_h + \mathbf{Q}$, this WF is equivalent to the Lee-Shih one [12]. Variational energies calculated vary with $\boldsymbol{q}_h$ [4,12]. The energy dispersions for t–J and t–t'–t''–J models are plotted as filled circles in Fig. 1(a) and (b), respectively. For both models, the ground state with one hole has momentum $(\pi/2,\pi/2) = \mathbf{Q}/2$. As shown in Ref. [4] and discussed briefly below, their dispersion relations are still followed when hole number is increased. The holes in these WF's behave just like quasi-particles (QP's), hence we denote $|\Psi_1(\boldsymbol{q}_h = \boldsymbol{q}_s)\rangle \equiv |\Psi_1^{QP}\rangle$.

As for the case of having an extra up-spin electron with momentum $\boldsymbol{q}_h$ doped into the half-filled state, the energy dispersion can be calculated with this same WF, $|\Psi_1^{QP}\rangle$. The

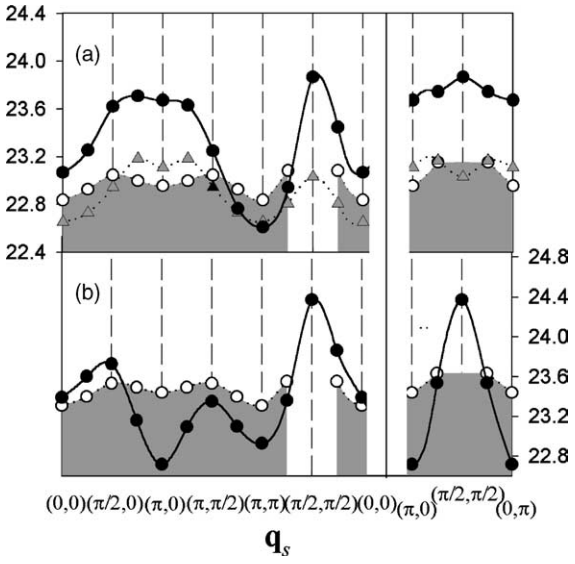

Fig. 1. Variational energies calculated for the (a) t–J and (b) t–t'–t''–J model Hamiltonians for one hole on an 8×8 lattice by applying our TWF's. Filled circles, connected by solid lines, are VMC results using the $|\Psi_1^{QP}(\mathbf{q}_s)\rangle$ discussed in the text; empty circles (gray triangles) by $|\Psi_1^{SB}(\boldsymbol{q}_s, \boldsymbol{q}_h = \mathbf{Q}/2((3\pi/4, 0))\rangle$. Shaded regions indicate a possible continuum for an infinite system. A minus sign has been multiplied to all the data shown here. Results are obtained with parameters $(\Delta/\chi, m_s, \chi) = (0.25, 0.125)$.

only difference is signs of t'/t and t''/t are changed in the Hamiltonian. This result agrees well with that obtained by SCBA [4]. The ground state is at momentum $(\pi/0)$. Both dispersions turn out to be simply the combination of the mean-field band at half-filling and the coherent hoppings [4,12]. Using $|\Psi_1^{QP}\rangle$, we calculated the momentum distribution function (MDF) $\langle n^h_\sigma(\mathbf{k})\rangle$ for the ground state of, say, a single 0$e$hole with momentum $\mathbf{Q}/2$. We observed the same dips or pockets at $\mathbf{Q}/2$ and *anti-dips* at -$\mathbf{Q}/2$ found for the exact results of 32 sites [4]. It is quite amazing that $|\Psi_1^{QP}\rangle$, including no t' and t'', not only produces the correct energy dispersions for a single doped hole or electron it also provides a correct picture about the momentum distribution.

To generalize the WF to describe states with more doped holes, we just take out the unpaired spin from $|\Psi_1^{QP}\rangle$ if we are interested in the state with zero total momentum and $S_z = 0$, which turns out to be the lowest energy state. For example, the TWF for two holes with momenta $\boldsymbol{q}_s$ and -$\boldsymbol{q}_s$ is

$$|\Psi_2\rangle = P_d \left[\sum_{\mathbf{k}\neq\pm\boldsymbol{q}_s} (A_{\mathbf{k}} a^\dagger_{\mathbf{k}\uparrow} a^\dagger_{-\mathbf{k}\downarrow} + B_{\mathbf{k}} b^\dagger_{\mathbf{k}\uparrow} b^\dagger_{-\mathbf{k}\downarrow}) \right]^{(N_s/2)-1} |0\rangle.$$

Note that the momentum $\boldsymbol{q}_s$ is not included in the summation. It is most surprising to find that although $|\Psi_2\rangle$ has zero total momentum irrespective of $\boldsymbol{q}_s$, its energy varies with the missing momentum or *the hole momentum* $\boldsymbol{q}_s$. For 2 electron doped case, the dispersion turns out to be very similar to that of a single doped electron [4]. The state with momentum $\boldsymbol{q}_s = (\pi,0)$ has the lowest energy for two electrons. Similarly, the energy dispersion for two holes doped into the half-filled state is also almost identical to that of a single hole and the

minimum is at **Q**/2 [4]. The lowest energy obtained is $-26.438(3)t$ for 8×8 system which is much lower than the variational energy, $-25.72(1)t$ [$-25.763(7)t$ when t' and t'' are included], using the TWF, say, applied by Himeda and Ogata [13] for 2 doped hole case. The MDF for this state has both dips at **Q**/2 and -**Q**/2. This is in good agreement with the exact result for the t–t'–t''–J model with 2 holes in 32 sites.

Applying the same type of TWF for four holes with momenta $\pm\mathbf{q}_s$ and $\pm\boldsymbol{q}_s^{'}$:

$$|\Psi_4\rangle = P_d\left[\sum_{\mathbf{k}\neq\pm\boldsymbol{q}_s,\pm\boldsymbol{q}_s^{'}}(A_{\mathbf{k}}a^{\dagger}_{\mathbf{k}\uparrow}a^{\dagger}_{-\mathbf{k}\downarrow}+B_{\mathbf{k}}b^{\dagger}_{\mathbf{k}\uparrow}b^{\dagger}_{-\mathbf{k}\downarrow})\right]^{(N_s/2)-2}|0\rangle,$$

where $\boldsymbol{q}_s^{'}$ and $\boldsymbol{q}_s$ are excluded from the summation, we can show our WF has AF LRO but very little superconducting pairing correlations. Fig. 2 shows that long range d-wave pairing correlation defined [14] for our TWF and that for Himeda-Ogata one. Thus the d-RVB pairing for spins assumed by our WF's does not imply the pairing of charges.

Computing the values of the staggered magnetization $m=N_s^{-1}\sum_i(-1)^i S_i^z$ at different dopings, we also found that the preference of having **Q**/2 for holes causes clearly larger disturbance of the AF order than for the electron doped case with momentum $(\pi/0)$ [4]. This is consistent with previous ED work and also the experimental results that AF phase is more stable for electron- than hole-doped case [16].

Clearly, the choice of unpaired spin to have the same momentum as the hole, i.e. $\boldsymbol{q}_s=\boldsymbol{q}_h$, is a special case for $|\Psi_1\rangle$. If we choose $\boldsymbol{q}_s\neq\boldsymbol{q}_h$, not only the electron pair at $\boldsymbol{q}_h$ and $-\boldsymbol{q}_h$ is excluded in the sum in $|\Psi_1\rangle$, the pair at $\boldsymbol{q}_s$ and $-\boldsymbol{q}_h$ is also affected. Hence we expect it to be higher in energy. To make a distinction from the afore-mentioned QP states $|\Psi_1^{\rm QP}\rangle$, these states will be denoted as the *spin-bag* (SB) states, i.e. $|\Psi_1(\boldsymbol{q}_s\neq\boldsymbol{q}_h)\rangle\equiv|\Psi_1^{\rm SB}\rangle$. The variational energies as a function of $\boldsymbol{q}_s$ for $|\Psi_1^{\rm SB}\rangle$ with $\boldsymbol{q}_h=\mathbf{Q}/2$ are plotted as empty circles in Fig. 1(a) and (b) for the t–J and t–t'–t''–J models. Many SB states could be constructed with the same $\boldsymbol{q}_s$ but different $\boldsymbol{q}_h$. While it is possible to have the SB states of even lower energy

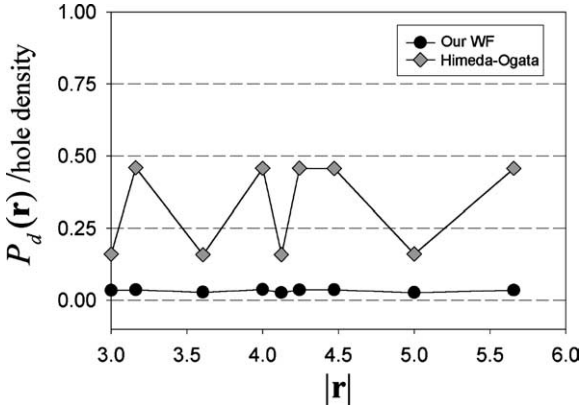

Fig. 2. d-wave pair–pair correlation function, $P_d(\mathbf{r})=(N_s)^{-1}\sum_i\langle\Delta_i^{\dagger}\Delta_{i+\mathbf{r}}\rangle$ where $\Delta_i=c_{i,\uparrow}(c_{i+\hat{x},\downarrow}+c_{i-\hat{x},\downarrow}-c_{i+\hat{y},\downarrow}-c_{i-\hat{y},\downarrow})$, with 4 doped holes in the 8×8 lattice. The result obtained using our WF is compared with that using the Himeda-Ogata WF (see text). Results here are obtained with optimized parameters $(\Delta/\chi,m_s,\chi)=(0.25,0.125)$ and, for Himeda-Ogata one, also $\mu=0.025$.

with $\boldsymbol{q}_h=(3\pi/4,0)$ in the t–J model (gray triangles in Fig. 1(a)), they are of higher energies than that of SB states with $\boldsymbol{q}_h=(\pi/2,\pm\pi/2)$ in the t–t'–t''–J case. There are many such states, actually an infinite number of them for an infinite system, forming a continuum, as schematically illustrated by the shaded regions in Fig. 1(a) and (b).

We then found that applying the spin operators $S^{\dagger(-)}(\mathbf{k}')=\sum_{q'}c^{\dagger}_{q'+\mathbf{k}'\uparrow(\downarrow)}c_{q'\downarrow(\uparrow)}$ to $|\Psi_1^{\rm QP}\rangle$, actually changes the QP state $|\Psi_1^{\rm QP}\rangle$ to the SB ones $|\Psi_1^{\rm SB}(\boldsymbol{q}_s=\boldsymbol{q}_h+\mathbf{k}')\rangle$. $\mathbf{k}'$ here represents thus the momentum of a linear spin wave. The particular term inlcuded in the sum of $\boldsymbol{q}'$ with $\boldsymbol{q}'$ equal to the momentum of the unpaired spin $\boldsymbol{q}_s=\boldsymbol{q}_h$ does the transformation. SB states are therefore just spin wave excitations of the QP state with the same hole momentum [5].

Because the unpaired spin is excited by the spin wave excitation and becomes unbound, the magnetization is suppressed around the hole for the SB state [5]. This is similar to the idea of a SB, thus the notation here, first proposed in Ref. [15].

A number of other physical properties associated with these two kinds of states are in good agreement with the exact results obtained by ED studies [5]. In particular, we obtained the drastic change of the spectral weight, $Z_{\mathbf{k}}=|\langle\Psi_1(\mathbf{k})|c_{\mathbf{k}\sigma}|\Psi_0\rangle|^2/\langle\Psi_0|c^{\dagger}_{\mathbf{k}\sigma}c_{\mathbf{k}\sigma}|\Psi_0\rangle$ as a QP state is switched to a SB one. For instance, with $|\Psi_1^{\rm QP}(\boldsymbol{q}=(\pi,0))\rangle$ we obtained $Z_{\mathbf{k}}=0.475$ but 0.0 when we use the SB state $|\Psi_1^{\rm SB}(\boldsymbol{q}_s=(\pi,0),\boldsymbol{q}_h=Q/2)\rangle$. This is consistent with exact results for the t–J model ($Z_{\mathbf{k}}=0.34$) and t–t'–t''–J model ($Z_{\mathbf{k}}=0$) [5]. By contrast, states at **Q**/2 and **Q**/4 remain to be QP states in both t–J and t–t'–t''–J models, hence large spectral weights are expected. In the presence of SB state, the overall variation pattern of spectral weights observed in the ARPES experiments on undoped parent compounds [1,2] may thus be naturally understood: notable lowest energy peaks are only observed in small regions of BZ, e.g. near **Q**/2 and $(\pi/2,0)$ where QP states have lower energy than the SB states (Fig. 1(b)).

Overdoped regime. Further increasing the density of doped holes or electrons in the t–t'–t''–J models, the WF described above is found to be switched to others with finite pairing amplitudes of charge carriers [6–8]. While it is difficult to show what occurs explicitly near the region of transition of our WF to others [7], we have found that, in optimal and overdoped regions, the replacing original d-RVB WF $|\Psi_{\rm RVB}\rangle=P_d\prod_{\mathbf{k}}(u_{\mathbf{k}}+v_{\mathbf{k}}c^{\dagger}_{\mathbf{k},\uparrow}c^{\dagger}_{-\mathbf{k},\downarrow})|0\rangle$, with the usual coherent factors $u_{\mathbf{k}}$ and $v_{\mathbf{k}}$, including t'/t, t''/t and chemical potential μ in the QP band, the pairing is greatly enhanced because of the deformation of the Fermi surface. The occupation number of $(\pi/0)$, increasing when t' and t'' are included, by electrons is important for this enhancement. The results [6] are similar to the conclusion of band structure calculations [17].

Focusing on the comparison with the ARPES results [3], we have also calculated the excitation spectrum of the RVB WF with odd numbers of electrons. Fig. 3 is the plot of the results at various dopings, compared with the experiments [8]. Also shown there, by applying the power-Lanczos method [18] the over-estimation of pairing in the variational approach is corrected to approach the experimental values [3].

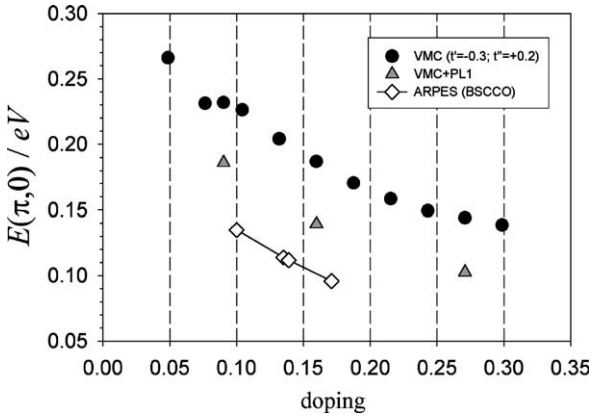

Fig. 3. Comparison of the excitation energy at $(\pi/0)$ calculated using the RVB WF, that after first order Lanczos method (VMC + PL1) and the experiments (see text). Note that the optimal doping determined by the RVB WF is around 0.30 and decreases as the WF is improved by PL1.

To sum up, we have thus discussed variational results for the low-energy states of the *t*–*J*-type models at different dopings. They reproduce various exact numerical results and, also, show consistent behaviors with what have been observed in the experiments.

Acknowledgements

We are grateful to the collaboration with N. Nagaosa, W.-C. Lee, P. W. Leung, R. Eder, C.-Y. Mou, Y. C. Chen, C.-P. Chou and S.-M. Huang which leads to work covered by this paper. Fruitful discussions with people in Z.-X. Shen and A. Fujimori's groups are greatly acknowledged.

References

[1] A. Damascelli, Z.-X. Shen, Z. Hussain, Rev. Mod. Phys. 75 (2003) 473.
[2] F. Ronning, et al., Phys. Rev. B 67 (2003) 165101 (for hole-doped systems); N.P. Armitage, et al., Phys. Rev. Lett. 88 (2002) 257001 (for electron-doped ones).
[3] K. Tanaka, et al., cond-mat/0312575; A. Fujimori, Private Communication.
[4] T.K. Lee, C.-M. Ho, N. Nagaosa, Phys. Rev. Lett. 90 (2003) 067001.
[5] W.-C. Lee, et al., Phys. Rev. Lett. 91 (2003) 057001.
[6] C.T. Shih, et al., Phys. Rev. Lett. 92 (2004) 227002.
[7] C.T. Shih, et al., cond-mat/0408422.
[8] T.K. Lee, C.-P. Chou, S.-M. Huang, work in progress.
[9] D.G. Clarke, Phys. Rev. B 48 (1993) 7520.
[10] T. Tohyama, S. Maekawa, Phys. Rev. B 49 (1994) 3596; R.J. Gooding, K.J.E. Vos, P.W. Leung, Phys. Rev. B 50 (1994) 12866.
[11] P.W. Anderson, Science 235 (1987) 1196.
[12] T.K. Lee, T. Shih, Phys. Rev. B 55 (1997) 5983.
[13] A. Himeda, M. Ogata, Phys. Rev. B 60 (1999) R9935.
[14] H. Yokoyama, M. Ogata, J. Phys. Soc. Jpn 65 (1996) 3615.
[15] J.R. Schrieffer, X.G. Wen, C. Zhang, Phys. Rev. Lett. 60 (1988) 944.
[16] H. Takagi, Y.S. Tokura, S. Uchida, Physica C 162–164 (1989) 1001; H. Takagi, Y. Tokura, S. Uchida, Phys. Rev. Lett. 62 (1989) 1197; G.M. Luke, et al., Phys. Rev. B 42 (1990) 7981; K. Yamada, et al., J. Phys. Chem. Solids 60 (1999) 102.
[17] E. Pavarini, et al., Phys. Rev. Lett. 87 (2001) 047003.
[18] C.T. Shih, et al., Phys. Rev. Lett. 81 (2001) 047003.